Sclerostin Antibody Administration Increases the Numbers of Sox9creER+ Skeletal Precursors and Their Progeny

Deepak H Balani, **Sophia Trinh**, **Mingxin Xu**, **Henry M Kronenberg**

Endocrine Unit, Massachusetts General Hospital and Harvard Medical School, Boston, MA, USA

Abstract

Blocking the Wnt inhibitor, sclerostin, increases the rate of bone formation in rodents and in humans. On a cellular level, the antibody against sclerostin acts by increasing osteoblast numbers partly by activating the quiescent bone-lining cells in vivo. No evidence currently exists, to determine whether blocking sclerostin affects early cells of the osteoblast lineage. Here we use a lineage-tracing strategy that uses a tamoxifen-dependent cre recombinase, driven by the Sox9 promoter to mark early cells of the osteoblast lineage. We show that, when adult mice are treated with the rat-13C7, an antibody that blocks sclerostin action in rodents, it increases the numbers of osteoblast precursors and their differentiation into mature osteoblasts in vivo. We also show that rat-13C7 administration suppresses adipogenesis by suppressing the differentiation of *Sox9creER + skeletal precursors into bone marrow adipocytes in vivo. Using floxed alleles of the *CTNNB1* gene encoding β-catenin, we show that these precursor cells express the canonical Wnt signaling mediator, β-catenin, and that the actions of the rat-13C7 antibody to increase the number of early precursors is dependent on direct stimulation of Wnt signaling. The increase in osteoblast precursors and their progeny after the administration of the antibody leads to a robust suppression of apoptosis without affecting the rate of their proliferation. Thus, neutralizing the Wnt-inhibitor sclerostin increases the numbers of early cells of the osteoblast lineage osteoblasts and suppresses their differentiation into adipocytes in vivo.

Keywords

SCLEROSTIN ANTIBODY; WNT SIGNALING; OSTEOBLAST PRECURSORS

Introduction

Wingless (Wnt) signaling pathways play an important role in regulating skeletal homeostasis during early embryonic development, postnatal development, and late adulthood.[1] in vitro experiments using osteogenic differentiation of skeletal stromal stem-like cells show that Wnt signaling is critical for the differentiation of multi-potent progenitor cells.[2] Studies of human diseases and in vivo animal experiments have shown the importance of Wnt signaling in determining bone mass and strength.[3] Wnt ligands consist of a group of 19 secreted glycoproteins that signal either through stabilization of β-catenin (canonical) or through non-canonical signaling pathways or both.[4]

Sclerostin protein, encoded by *SOST* gene, is produced by osteocytes, and the protein is known to negatively regulate bone formation by suppressing Wnt signaling. Mutations around the *SOST* gene are known to give rise to certain human skeletal dysplasias such as sclerosteosis and van Buchem disease.[1] Manipulations that increase bone formation, including intermittent parathyroid hormone (PTH) administration and mechanical loading, do so in part by reducing sclerostin protein production in osteocytes.[5, 6] On a cellular level, sclerostin protein is known to inhibit bone formation by affecting osteoblasts.[4, 5] For example, Kim and colleagues used a lineage tracing strategy to show that sclerostin-antibody could act on bone lining cells in vivo to stimulate these cells to become osteoblasts.[7] However, the precise molecular mechanisms through which sclerostin regulates early cells of the osteoblast lineage remain incompletely understood. Until recently, identifying such unique cells in vivo has been particularly challenging. Inability to identify such cells in vivo made it difficult to study the role of Wnt signaling in such skeletal precursors.

Bone marrow contains stromal/mesenchymal cells that can form colonies in culture (CFU-Fs). Within these CFU-Fs lie cells that exhibit multi-potential behavior, ie, capability to differentiate into osteoblasts, chondrocytes, stromal cells, and adipocytes in vitro.[8, 9] However, their normal in vivo fates remain elusive, as specific marking of such cells in vivo has proven challenging. Recently, several groups have used a variety of transgenes to mark such cells in vivo. Promoters such as those for nestin, α smooth muscle actin,[10] MX1 stimulated with polyI-polyC,[11] gremlin[12] leptin receptor,[13] Gli-1[14] and Ebf3[15] have been used to identify osteoblast precursors in vivo. To identify fetal, early postnatal and adult stromal cells capable of differentiating into chondrocytes, adipocytes, and osteoblasts, we have used *Sox9*-cre/ERT2 to mark such cells.[16, 17]

The ability to mark early cells of the osteoblast lineage and follow them allows us to study the effects of Wnt inhibitors on osteoprogenitors to increase bone mass. In this study, we utilize transgenic mice expressing *Sox9*-cre/ERT2; *R26R*-Tomato reporter and a constitutively active Osteocalcin-GFP (OcnGFP) mouse to study the effect of sclerostin antibody administration on these skeletal precursors and their differentiation into osteoblast lineage. We show how sclerostin antibody directly affects skeletal precursors by changing their rate of apoptosis and driving them into the osteoblastic lineage in vivo.

Materials and Methods

Mice

To determine the cell fate of *Sox9*-expressing cells in response to anti-sclerostin antibody treatment (RC-317), transgenic mice were generated from Sox9-*creER*^{T226} (H Akiyama),[18] *Rosa26-loxP-stop-loxP*-tdTomato (*R26R*-tomato, JAX7914), C57BL/6-Tg (BGLAP-Topaz)1Rowe/J (*Ocn*-GFP/tpz, JAX17469), and B6.129-*Ctnnb1*^{tm2Kem}/KnwJ (JAX4152) mice. All mice were back-crossed into C57BL/6J inbred mice (JAX664) for at least 10 generations. Mice were identified by nickel-copper ear tags supplied by the National Band & Tag Company (Newport, KY, USA). To label skeletal precursors marked by *Sox9*, tamoxifen (Sigma-Aldrich, St. Louis, MO, USA; T5648–1G) was dissolved in 100% ethanol and subsequently mixed in sunflower seed oil (Sigma-Aldrich, S5007). This mixture was incubated at 60°C overnight for ethanol to evaporate completely before use. Unless otherwise stated, mice at postnatal day 42 were given intraperitoneal administration of 2 mg of tamoxifen. After 24 hours, mice were given either once-weekly subcutaneous injections of anti-sclerostin antibody (RC-317) at 100 mg/kg (Amgen, Thousand Oaks, CA, USA) or weekly subcutaneous injections of vehicle (10 mM sodium acetate from glacial acetic acid, 9% sucrose, 0.004% PS 20, pH 5.0) for 3 days, 7 days, 21 days, 4 weeks, or 8 weeks before euthanization.

During this experimental period, mice were housed in a pathogen-free, temperature- and humidity-controlled facility with husbandry maintained and provided by the Center of Comparative Medicine at the Massachusetts General Hospital.

Polymerase chain reaction

Tissue samples were collected from 6.35 mm tail biopsies and incubated overnight in an alkaline lysis reagent (1 M Tris [pH 8.0], 5 M NaCl, 0.5 M EDTA, 20% sodium dodecyl sulfate [SDS], Millipore H_2O) mixed with crude proteinase K (Sigma-Aldrich, P8044–1G). Genotyping was performed by PCR (Peltier Thermal Cycler, PTC-200) using GoTaq Green Master Mix (VWR International, Radnor, PA, USA; PAM7123). DNA samples (10 μL) were pipetted into each well of a 2% agarose gel (Thermo Fisher Scientific, Waltham, MA, USA; 16500500) and stained with ethidium bromide. The electrophoresis was performed in 1x TAE buffer (Tris [Tromethamine], glacial acetic acid, 0.5 M EDTA).

Histology

The anesthetic drug isoflurane (Piramal, Lexington, KY, USA) was used to euthanize mice. Severance of the high cervical spinal column was performed to ensure death. Hindlimbs were dissected, and the tibias and femurs were harvested in accordance to standard published protocols and then fixed in 4% paraformaldehyde or 10% neutral-buffered formalin (NBF). Samples were incubated at 4°C overnight followed by decalcification with 15% EDTA mixed in Millipore water for a period ranging from 14 to 21 days. Decalcified samples were placed in 30% sucrose/PBS solution for 24 hours and then transferred into 30% sucrose/PBS:OCT (1:1) solution for cryoprotection. Prepared samples were embedded in OCT compound (Sakura Finetek, Torrance, CA, USA; 4583) and cryosectioned at 15 μm

via Shandon Cryotome SM. Long-term storage of frozen formalin-fixed tissue sections was at −20°C.

Microscopy

Multicolor images were obtained using 2× and 10× eyepieces and were captured using an epifluorescence microscopy (Nikon [Tokyo, Japan] Eclipse). The epifluorescence microscope was configured with triple-band filter settings of DAPI/FITC/TRITC and images were captured on a Mac Desktop (Apple Inc., Cupertino, CA, USA) with a 4× objective from Nikon and acquired using a SPOT Advanced Imaging Software (v.5.2). Confocal images were generated with LSM710 and ZenBlack Software (Zeiss, Thornwood, NY, USA) using lasers and corresponding band-pass filters for DAPI (Ex. 405 nm), FITC (Ex. 488 nm), and Tomato (Ex. 543 nm). An LSM Image Viewer was used to capture, align, and generate a representative image. Each panel reflects data from three mice/genotype from three independent experiments. Routine H&E was used for histology, and oil red O staining was used to visualize adipocytes and was performed using previously published protocols.

Flow cytometry

Limbs were carefully dissected and femurs were harvested and gently crushed in 2 mL of HBSS (Sigma-Aldrich, H6648–1L) with a mortar and pestle (CoorsTek, Golden, CO, USA). Each crushed femur was given 2 Wunsch units (77 μL per unit) of Liberase (Thermo Fisher Scientific, 501004934) and 200 μL of 0.5% Trypsin–EDTA (Sigma-Aldrich, T7168–20TAB) and placed on a shaking incubator (Eppendorf [Hamburg, Germany] Thermomixer R) for 30 minutes at 37°C. Isolated cells were filtered into 50-mL Falcon tubes and the remaining bone was mechanically triturated with a 1-mL syringe (BD Biosciences, San Jose, CA, USA) and 18-gauge needle. The tissue remnants were digested again in 2 Wunsch units of Liberase and 200 μL of 0.5% Trypsin–EDTA for 30 minutes at 37°C before the tubes were placed into a centrifuge (Eppendorf Centrifuge 5810 R) for 25 minutes at 1450 rpm and 4°C. The supernatant was discarded, and the resultant pellet was suspended in 400 μL of 1:250 anti-CD45-APC (Thermo Fisher Scientific, 5014971) for 30 minutes on ice in a darkroom. After staining, the cells were washed with 2 mL Dulbecco's PBS (DPBS) with 2% fetal bovine serum (FBS) for 10 minutes and spun at 1200 rpm. The supernatant was discarded after centrifugation and the stained cells were resuspended in DPBS with 2% FBS before performing flow cytometry. The 4-laser BD LSRII (Ex. 355/407/488/633 nm) flow cytometer was used to run samples and analyzed using FACS-DIVA software. Data were transferred to a Mac desktop computer as .fcs files and then used to generate dot plots using FlowJo software (TreeStar, Ashland, OR, USA). Data shown are representative plots of at least three independent experiments as previously described.[17]

Cell proliferation and apoptosis assays

Assessment of cell proliferation was performed by administering 5-ethynyl-2′-deoxyuridine (EdU) (Life Technologies Corporation, A10044) intraperitoneally to adult mice. Each mouse received a total of 1.5 mg of EdU dissolved in PBS in three divided doses at 2-hour intervals over 6-hours and then sacrificed. Cells were isolated as described above in the flow cytometry section. Evaluation of EdU-positive cells was performed using Click-iT Imaging Kit with Alexa Fluor 488 Assay Kit (Life Technologies Corporation, Carlsbad, CA, USA;

C10632). To quantify apoptotic cells, tibias and femurs were harvested from adult mice and stained with 1:250 anti-CD45-APC (eBioscience, San Diego, CA, USA; 17–0451–82) and Ter119-APC (eBioscience, 17–5921–82) followed by staining with FITC Annexin V Apoptosis Detection Kit (BioLegend, San Diego, CA, USA; 640922) for 15 minutes. The rate of apoptosis was measured and evaluated under flow cytometry using an LSR II flow cytometer.

Micro-CT

To assess accumulation of adipocytes in the bone marrow, tibias of RC-317- and vehicle-treated mice were harvested and fixed in 10% neutral buffered formalin (NBF) for 24 hours at 4°C. The mineralized bones were processed by the micro-CT (μCT) core at the Center for Skeletal Research, Massachusetts General Hospital, and bone morphology parameters were obtained. Samples were subsequently decalcified in EDTA 15 days and stained with osmium tetroxide (5% potassium dichromate and 2% osmium tetroxide mixture in 15-mL conical tube) for 48 hours before visualizing and quantifying marrow adipose tissue by μCT (SCANCO Medical, Brüttisellen, Switzerland).

Study approval

All studies were conducted in compliance with the Standard Operating Procedures for the Care and Use of Laboratory Animals, which has been approved by the Institutional Animal Care and Use Committee (IACUC) of Massachusetts General Hospital.

Statistics

Results shown here are represented as ±SEM. Statistical evaluation was performed using a nonparametric two-tailed Student's t test using GraphPad Prism version 7 for Mac (www.graphpad. com, La Jolla, CA, USA). Data represent mean ± SEM from three independent experiments with three mice/experiment).

Results

Blocking sclerostin by administering rat-13C7 antibody increases the numbers of Sox9creER+ skeletal precursors and their progeny in vivo

To determine whether the antibody against sclerostin, administered subcutaneously as once-weekly injection affected *Sox9*-creERT2-expressing precursors and their descendants, we pulsed mice on postnatal day 42 (P42) with a 2-mg dose of tamoxifen and 24 hours later began administering antibody or vehicle weekly; we euthanized the mice at 3, 7, and 21 days after tamoxifen administration (Fig. 1A). Three days after tamoxifen, we observed cells expressing tdTomato in the chondrocytes of growth plate cartilage, in cells of the primary and secondary spongiosa (called "spongiosa" subsequently), and in cells on the endocortical and periosteal surfaces in both vehicle- and antibody-treated mice (Fig. 1B, E). TdTomato-expressing cells present in the spongiosa (Supplemental Fig. S3A, D) or on the cortical bone of the diaphysis (Supplemental Fig. S4A, D) did not change 3 days after antibody treatment (see Supplemental Fig. S2 for the definition of the spongiosa and cortical regions of the tibia counted throughout this article). After tamoxifen administration on day 3, we observed 4.23 ± 0.4 tdTomato+cells/section in the spongiosa of vehicle-administered mice compared with

5.33 ± 1.52 cells/section in mice that received the antibody (Fig. 1H). Similarly, endocortical and periosteal tdTomato+ cells showed no significant difference in numbers (13.33 ± 7.63/ section versus 12 ± 5.56/section) (Fig. 1I). However, by day 7, the antibody caused striking differences in the cortex of the antibody-treated group compared with vehicle-treated animals. The tdTomato+ cells in the spongiosa (34.67 ± 24.66/section versus 51 ± 7/section) showed no significant changes (Supplemental Fig. S3B, E and Fig. 1H). However, there was a significant increase in the tdTomato+ population associated with the cortical bone (14.66 ± 2.88/section versus 55 ± 6.35/section) in Sclerostin antibody (Scl-ab)-treated mice (Supplemental Fig. S4B, E and Fig. 1I). On day 21, the mice that received Scl-ab showed an overall increase in their tdTomato+ population (Fig. 1G, arrows) in comparison to that in vehicle-treated mice (Fig. 1D). Higher numbers of spongiosa tdTomato + cells were observed in the antibody-treated animals (Supplemental Fig. S3F, asterisk) (60.33 ± 40.46/ section versus 195 ± 25.70/section) compared with controls (Fig. 1H). Similarly, the cortical bone showed a significant increase in the number of tdTomato+ cells in the antibody-treated animals (Supplemental Fig. S4F, C; Fig. 1I) (21.66 ± 10.06/section versus 40 ± 5.19/ section). We observed that several Sox9creER+ cells were embedded deep inside the cortical bone that resembled osteocytes. Furthermore, to determine whether the antibody affected the number of early *Sox9*-creERT2-positive cells, the transgenic mice received either Scl-ab or vehicle for either 3 or 7 days, followed by tamoxifen administration to each group. Twenty-four hours later, mice were euthanized (see scheme in Supplemental Fig. S1). We observed that at all time points, the antibody-treated mice showed a higher number of non-growth plate tdTomato+ cells compared with vehicle-treated mice, but this difference only became significant after 7 days of antibody treatment (0.069% in vehicle versus 0.19% in Scl-ab; Supplemental Fig. S1). These findings suggest that blocking the action of the Wnt-inhibitor sclerostin augments the number of *Sox9*-creERT2+ mesenchymal precursors in vivo.

Blocking sclerostin action leads to an increase in the numbers of differentiated Sox9creER + osteochondral precursors in vivo

To assess whether the administration of the antibody affected the numbers of non-growth plate tdTomato+ cells that differentiated into mature osteoblasts, Sox9-creER; R26RTomato mice were crossed to mice that constitutively expressed green fluorescent protein (GFP) under the control of the osteocalcin promoter. On day 3 after tamoxifen administration, sections did not show any significant differences in the numbers of differentiated cells in mice treated with either vehicle or antibody (4.33 ± 3.21 tdTomato+ and GFP cells/section versus 3 ± 1.73/section in the spongiosa and 7.66 ± 4.72/section versus 4.33 ± 2.3/section in cortical bone) (Fig. 2B, E, H, I). In vehicle-treated mice, cells remained largely undifferentiated and did not show any overlap with GFP in both the spongiosa (Supplemental Fig. S5A, D) and cortical bone (Supplemental Fig. S6A, D). However, we observed that the higher number of tdTomato+ population co-localized with GFPtpz fluorescence on day 7, indicating an increased number of differentiated tdTomato+ cells in antibody-treated mice present in the spongiosa (8.67 ± 3.51 versus 27.67 ± 1.52) (Supplemental Fig. S5B, E) and cortical bone (7.66 ± 4.16 versus 14 ± 1.73) (Supplemental Fig. S6B, E). The results were striking on day 21; Sox9-creER; R26RTomato cells that differentiated into mature osteocalcin-expressing osteoblasts were significantly higher in number in the spongiosa (18 ± 8.71 versus 70.67 ± 31.64) (Supplemental Fig. S5C, F; Fig.

2H) and the cortical bone (7 ± 3.6 versus 16.33 ± 7.5) (Supplemental Fig. S6C, F; Fig. 2I); the tdTomato+ cells also showed an increased differentiation into osteocytes in the antibody-treated mice compared with vehicle-treated mice (Supplemental Fig. S6F). These results suggest that blocking sclerostin not only augments the number of Sox9-creER+ cells but also increases the numbers of mature osteoblasts differentiated from Sox9-creER; R26RTomato + cells in vivo.

Blocking sclerostin action suppresses the rate of apoptosis of Sox9creER+ skeletal precursors and their progeny without affecting their rate of proliferation in vivo

To assess if the antibody stimulated proliferation of Sox9creER+ cells, the Sox9-creER; R26RTomato mice were administered 0.5 mg of EdU intraperitoneally thrice in the interval of 2 hours before euthanization after treatment with either vehicle or a single dose of the antibody given 24 hours after administration of tamoxifen (Fig. 3A). Bone marrow hemopoietic cells and erythroid cells were gated out using anti-CD45 and anti-Ter119 antibody, respectively. No significant differences were found in the rate of proliferation between antibody-treated mice and controls (10.08% ± 0.52% versus 8.08% ± 1.49%) (Fig. 3B, C). We utilized a commercially available Annexin V-FITC staining kit to assess the rate of apoptosis in the Sox9-creER; R26RTomato + cells. Hematopoietic cells and dead cells were gated out by anti-CD45/Ter-119 antibody and DAPI staining, respectively. We detected a significant suppression in the rate of apoptosis of the Sox9-creER; R26RTomato + population in the Scl-ab-treated animals compared with vehicle-treated mice on day 7 (antibody: 15.08% ± 2.23% versus veh: 22.33 ± 0.44%) (Fig. 3D, E). Thus, Scl-ab regulates the number of Sox9-creER+ mesenchymal precursors by suppressing their rate of apoptosis without changing their rate of proliferation in vivo.

Conditional knock-out of β-catenin in Sox9creER+ cells abrogates the effects of blocking sclerostin action on Sox9creER+ skeletal precursors and their progeny in vivo

To determine whether the mechanism of Scl-ab-mediated increase in Sox9creER+ cells is via direct activation of Wnt-β-catenin signaling or via indirect mechanisms, we generated Sox9-creER; R26RTomato; β-catenin $^{fl/fl}$ transgenic mice. After tamoxifen administration, this model permits concurrent labeling of cells expressing Sox9creER with tdTomato and deletion of the gene that encodes β-catenin.

Sox9-creER; R26RTomato; β-catenin $^{fl/fl}$ transgenic mice and Sox9-creER; R26RTomato; β-catenin $^{wt/wt}$ (3 in each group) received 2 mg tamoxifen and then received either vehicle or Scl-ab antibody once, 24 hours after administration of tamoxifen. In Sox9-creER; β-catenin $^{wt/wt}$ mice, after antibody administration, cortical bone showed a significant increase in the number of Sox9-creER; tdTomato+ cells compared with controls (25.16 ± 2.75 [vehicle] versus 53.6 ± 5.77 [antibody], $p < .01$). However, deletion of β-catenin caused a complete abrogation of increase in the number of cortical tdTomato+ cells (10.6 ± 6.42 (vehicle) versus 7.6 ± 2.51 (antibody) after antibody administration (Fig. 4B–E, Supplemental Fig. S7A–H). We also observed very similar results with flow cytometry analysis (Fig. 4F). We observed significant increase in the number of tdTomato+ cells after antibody administration in Sox9-creER; R26RTomato; β-catenin $^{wt/wt}$ mice compared with controls ($1.8 \times 10^{-3} \pm 3.54 \times 10^{-4}$ [vehicle] versus $7.8 \times 10^{-3} \pm 6.3 \times 10^{-4}$ [antibody]). In contrast, after ablation

of β-catenin expression in these cells using Sox9-creER; R26RTomato; β-catenin $^{fl/fl}$ mice, we observed no significant difference in the cellular response to vehicle or antibody ($1 \times 10^{-3} \pm 3.5 \times 10^{-4}$ [vehicle] versus $2.2 \times 10^{-3} \pm 2.8 \times 10^{-4}$ [antibody]) (Fig. 4F). Thus, knocking β-catenin from Sox9-creER+ mesenchymal precursors abrogated the effects of antibody administration, suggesting that the antibody acts directly on the Sox9-creER+ skeletal precursors and their progeny in vivo.

Blocking sclerostin action regulates the fates of skeletal precursors by suppressing adipogenic differentiation of skeletal precursors in vivo

To determine if blocking sclerostin action affects the fates of skeletal precursors, we administered a single 2-mg dose of tamoxifen intraperitoneally followed by a once-weekly subcutaneous administration of 50 mg/kg antibody for 8 weeks (Fig. 5A). Marrow adipogenesis was assessed in the proximal tibia using osmium tetroxide staining as previously described (Fig. 5B, D).[18] Similarly, mineralized bone was assessed in the same mice using micro-CT (Fig. 5C, E). Antibody administration decreased the number of marrow adipocytes in the proximal tibia (Fig. 5B, D) and distal tibia (Fig. 5F, G), probably by decreasing marrow adipogenesis. Adipocytes labeled by osmium tetroxide were significantly fewer in the antibody-treated mice (Fig. 5D) than in the vehicle-treated mice (Fig. 5B). Furthermore, to investigate if the antibody affected the differentiation of Sox9creER; R26RTomato + skeletal precursors and their progeny, we administered a single 2-mg dose of tamoxifen intraperitoneally followed by once-weekly subcutaneous administration of 50 mg/kg antibody for 8 weeks and stained the frozen sections with anti-perilipin antibody to detect the fraction of Sox9creER; R26RTomato + that had differentiated into adipocytes in vivo (Fig. 5H, I). The fraction of Sox9creER; R26RTomato + marrow cells that were adipocytes and the total number of adipocytes were significantly smaller in antibody-treated animals than in vehicle-treated mice (Fig. 5J, K).

Discussion

Here we used lineage tracing to show that Scl-Ab can increase the number of osteoblast precursors and osteoblasts in vivo. This result corroborates previous stereological data that demonstrated that administration of Scl-ab leads to an increase in Runx2-positive cells, a fraction of which is likely to be osteoprogenitors, and concomitant increase in osteoblast numbers.[19]

Other anabolic drugs such as teriparatide also augment Sox9creER+ osteoblast precursors and their progeny in vivo. Teriparatide has been shown to lower sclerostin levels in bone;[17] therefore, it is possible that PTH-mediated increase in skeletal precursors could also occur partly via reducing sclerostin production by osteocytes in vivo.

We also demonstrate that Scl-Ab action did not alter the rate of proliferation of tomato+ cells but significantly suppressed the rate of apoptosis in those, a mechanism very similar to that of teriparatide as shown previously. We also showed that the action of the antibody requires the presence of beta-catenin in osteoblast precursors to increase the number of tomato+ cells. Deletion of β-catenin in Sox9creER+ osteoblast precursors led to complete abrogation of the increase in Sox9creER+ cell number after antibody administration.

Previous investigators have shown that beta-catenin is absolutely required for the generation of osteoblasts during development,[20] mediates the action of VEGF to increase bone mass, [22] and has crucial roles during the transition from hypertrophic chondrocytes to osteoblasts in the primary spongiosa.[23] Further, in mature osteoblasts, beta-catenin action leads to an increase in osteoprotegerin production and a suppression of osteoclasts.[21] The suppression of sclerostin here, by increasing canonical Wnt signaling, can thus have multiple effects that could contribute to the increase in osteoblast precursors and their progeny that we see here. Which Wnts target osteoblast precursors and the cellular source of these Wnts is an important question for future analysis.

The anabolic bone-forming ability of intermittent PTH and Scl-ab administration decreases with time.[24, 25] A pleasing hypothesis that might partly account for this phenomenon could be that prolonged usage of these anabolic drugs might lead to an eventual decrease in the pool of skeletal precursors poised to become osteoblasts; this hypothesis requires further study.

Osteoblast precursors are capable of differentiating into osteoblasts, adipocytes, and reticular cells.[8] Activation of the Wnt signaling pathway suppresses peroxisome proliferator activated receptor-gamma, a crucial transcription factor that leads to adipocytic differentiation of mesenchymal stem cells in vitro and in vivo.[26] This action probably contributes to our finding that the conversion of Sox9creER+ cells to adipocytes is decreased after Scl-ab administration. A similar action may be involved in PTH action, as well. We recently showed that PTH 1–34 (teriparatide) withdrawal, after administration of teriparatide in an anabolic protocol, leads to an increase in adipocyte number and a decrease in the activated form of β-catenin and that, conversely, teriparatide administration suppresses adipocytic differentiation of Sox9creER+ cells in vivo.[17] Whether this effect is a result of an increase in sclerostin secretion from osteocytes needs further exploration.

Supplementary Material

Refer to Web version on PubMed Central for supplementary material.

Acknowledgments

References

1. Krishnan V, Bryant HU, MacDougald OA. Regulation of bone mass by Wnt signaling. J Clin Invest. 2006;116(5):1202–9. [PubMed: 16670761]

2. Abdallah BM, Jafari A, Zaher W, Qiu W, Kassem M. Skeletal (stromal) stem cells: an update on intracellular signaling pathways controlling osteoblast differentiation. Bone. 2015;70:28–36. [PubMed: 25138551]

3. Baron R, Kneissel M. WNT signaling in bone homeostasis and disease: from human mutations to treatments. Nat Med. 2013;19(2):179–92. [PubMed: 23389618]

4. MacDonald BT, Tamai K, He X. Wnt/β-catenin signaling: components, mechanisms, and diseases. Dev Cell. 2009;17(1):9–26. [PubMed: 19619488]

5. Keller H, Kneissel M. SOST is a target gene for PTH in bone. Bone. 2005;37(2):148–58. [PubMed: 15946907]

6. Bellido T, Ali AA, Gubrij I, et al. Chronic elevation of parathyroid hormone in mice reduces expression of sclerostin by osteocytes: a novel mechanism for hormonal control of osteoblastogenesis. Endocrinology. 2005;146(11):4577–83. [PubMed: 16081646]

7. Kim SW, Lu Y, Williams EA, et al. Sclerostin antibody administration converts bone lining cells into active osteoblasts. J Bone Miner Res. 2017;32(5):892–901. [PubMed: 27862326]

8. Owen M, Freidenstein A. Stromal stem cells: marrow derived osteogenic precursors. Ciba Found Symp. 1988;136:42–60. [PubMed: 3068016]

9. Bianco P, Robey PG, Simmons PJ. Mesenchymal stem cells: revisiting history, concepts, and assays. Cell Stem Cell. 2008;2(4):313–9. [PubMed: 18397751]

10. Kalajzic Z, Li H, Wang L-P, et al. Use of an alpha-smooth muscle actin GFP reporter to identify an osteoprogenitor population. Bone. 2008; 43(3):501–10. [PubMed: 18571490]

11. Park D, Spencer JA, Koh BI, et al. Endogenous bone marrow MSCs are dynamic, fate-restricted participants in bone maintenance and regeneration. Cell Stem Cell. 2012;10(3):259–72. [PubMed: 22385654]

12. Worthley DL, Churchill M, Compton JT, et al. Gremlin 1 identifies a skeletal stem cell with bone, cartilage, and reticular stromal potential. Cell. 2015;160(1–2):269–84. [PubMed: 25594183]

13. Zhou BO, Yue R, Murphy MM, Peyer JG, Morrison SJ. Leptin-receptor-expressing mesenchymal stromal cells represent the main source of bone formed by adult bone marrow. Cell Stem Cell. 2014;15(2):154–68. [PubMed: 24953181]

14. Shi Y, He G, Lee W-C, McKenzie JA, Silva MJ, Long F. Gli1 identifies osteogenic progenitors for bone formation and fracture repair. Nat Commun. 2017;8(1):2043. [PubMed: 29230039]

15. Seike M, Omatsu Y, Watanabe H, Kondoh G, Nagasawa T. Stem cell niche-specific Ebf3 maintains the bone marrow cavity. Genes Dev. 2018;32(5–6):359–72. [PubMed: 29563184]

16. Ono N, Ono W, Nagasawa T, Kronenberg HM. A subset of chondrogenic cells provides early mesenchymal progenitors in growing bones. Nat Cell Biol. 2014;16(12):1157–67. [PubMed: 25419849]

17. Balani DH, Ono N, Kronenberg HM. Parathyroid hormone regulates fates of murine osteoblast precursors in vivo. J Clin Invest. 2017;127(9):3327–38. [PubMed: 28758904]

18. Soeda T, Deng JM, De Crombrugghe B, Behringer RR, Nakamura T, Akiyama H. Sox9-expressing precursors are the cellular origin of the cruciate ligament of the knee joint and the limb tendons. Genesis. 2010;48(11):635–44. [PubMed: 20806356]

19. Ominsky MS, Brown DL, Van G, et al. Differential temporal effects of sclerostin antibody and parathyroid hormone on cancellous and cortical bone and quantitative differences in effects on the osteoblast lineage in young intact rats. Bone. 2015;81:380–91. [PubMed: 26261096]

20. Hill TP, Später D, Taketo MM, Birchmeier W, Hartmann C. Canonical Wnt/β-catenin signaling prevents osteoblasts from differentiating into chondrocytes. Dev Cell. 2005;8(5):727–38. [PubMed: 15866163]

21. Glass DA, Bialek P, Ahn JD, et al. Canonical Wnt signaling in differentiated osteoblasts controls osteoclast differentiation. Dev Cell. 2005;8(5):751–64. [PubMed: 15866165]

22. Maes C, Goossens S, Bartunkova S, et al. Increased skeletal VEGF enhances B-catenin activity and results in excessively ossified bones. EMBO J. 2010;29(2):424–41. [PubMed: 20010698]

23. Houben A, Kostanova-Poliakova D, Weissenböck M, et al. β-catenin activity in late hypertrophic chondrocytes locally orchestrates osteoblastogenesis and osteoclastogenesis. Development. 2016;143(20):3826–38. [PubMed: 27621061]

24. Gatti D, Viapiana O, Idolazzi L, Fracassi E, Rossini M, Adami S. The waning of teriparatide effect on bone formation markers in postmenopausal osteoporosis is associated with increasing serum levels of DKK1. J Clin Endocrinol Metab. 2011;96(5):1555–9. [PubMed: 21367927]

25. McClung MR, Brown JP, Diez-Perez A, et al. Effects of 24 months of treatment with romosozumab followed by 12 months of denosumab or placebo in postmenopausal women with low bone mineral density: a randomized, double-blind, phase 2, parallel group study. J Bone Miner Res. 2018;33(8):1397–406. [PubMed: 29694685]
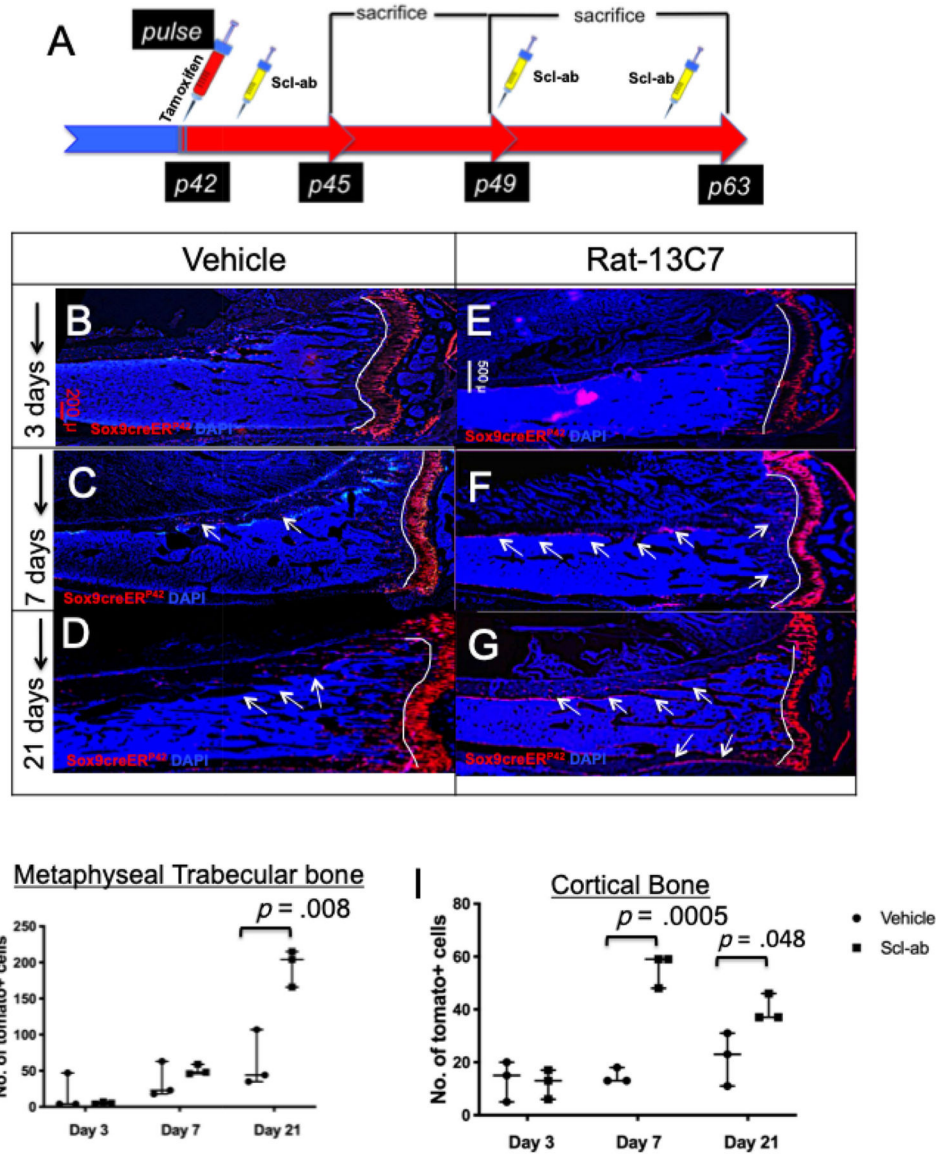
26. Spiegelman BM, Hu E, Kim JB, Brun R. PPAR gamma and the control of adipogenesis. J Control Release. 1997;79(2–3):111–2.

Fig 1.

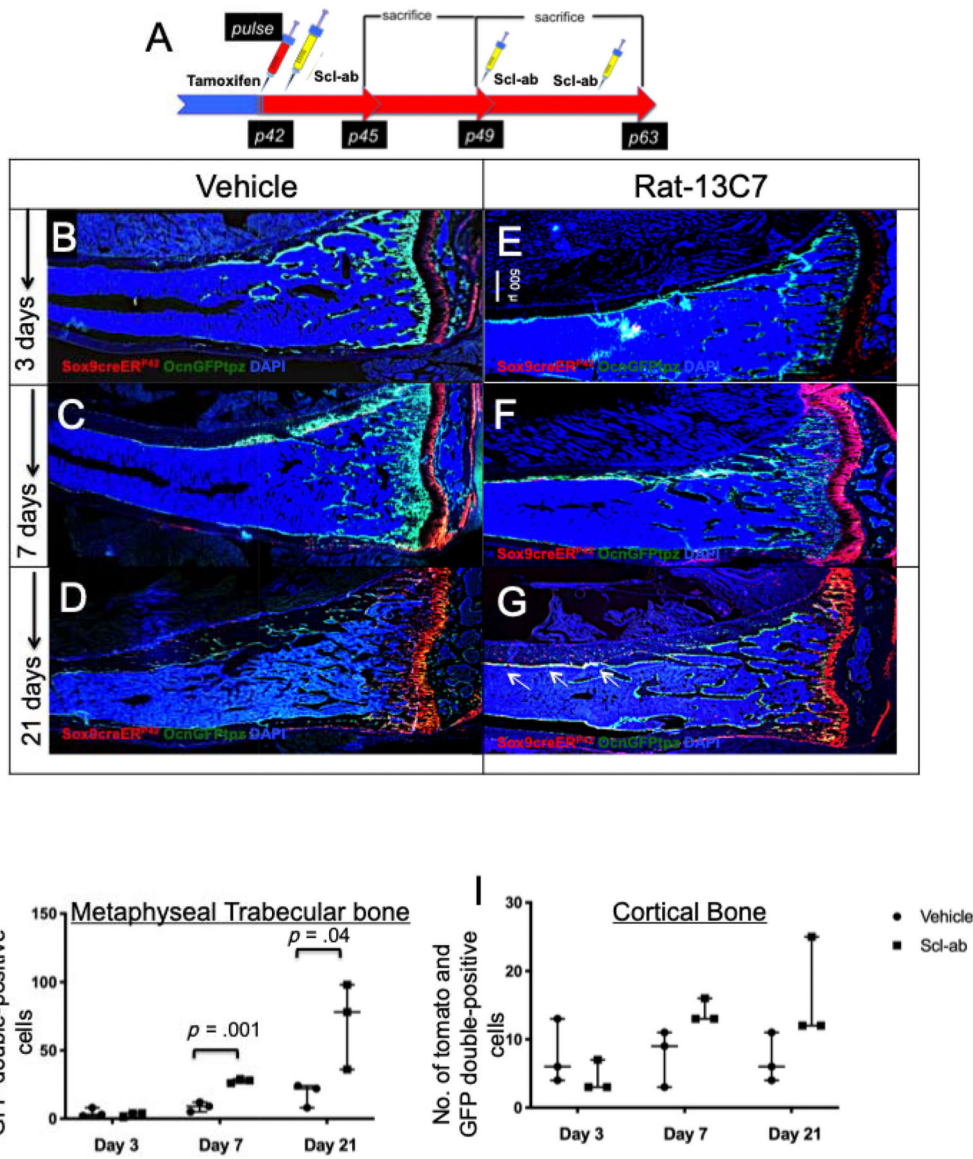Blocking sclerostin increases the numbers of Sox9creER; R26RTdTomato + cells and its descendants in vivo. (*A*) The experimental protocol used to study the modulation of numbers of Sox9-creER+ cells. Mice were administered a single dose of tamoxifen (red syringe) at P42 intraperitoneally. Twenty-four hours later, mice were given either vehicle or rat-13C7 antibody against sclerostin protein, once weekly (yellow syringes). Mice were euthanized at 3, 7, and 21 days after tamoxifen administration, and tibias were harvested for evaluation by epifluorescence microscopy of whole bone (*B–G*). Representative sections from Sox9creER; R26RTdTomato; mice at 3 days (*B, E*), 7 days (*C, F*), and 21 days (*D, G*) post-tamoxifen administration. (*H, I*) The number of Sox9creER-R26RTdTomato + cells counted blindly as previously in the spongiosa and in the diaphysis of cortical bone counted in a standard region described in Supplemental Fig. S2 on days 3, 7, and 21 after tamoxifen administration in vehicle- and antibody-administered mice.

Fig 2.

Blocking sclerostin action increases differentiation of Sox9creER; OcnGFPtpz; R26RTdTomato + cells and mature osteoblasts in vivo. (*A*) The protocol used to study the rate of differentiation of numbers of Sox9-creER+ cells and their descendants. A single 2-mg dose of tamoxifen was administered at P42. Twenty-four hours later, mice were subjected to vehicle or rat-13C7 antibody against sclerostin protein, once weekly, and mice were euthanized 3, 7, and 21 days after tamoxifen administration. Mice were euthanized and long bones were harvested and evaluated by epifluorescence microscopy (*B–G*). Representative long bone section from Sox9creER; R26RTdTomato; OcnGFPtpz mice at 3 days (*B, E*), 7 days (*C, F*), and 21 days (*D, G*) post-tamoxifen administration. (*H, I*) The number of Sox9creER-R26RTdTomato/OcnGFPtz double+ cells counted blindly in the spongiosa and cortical bone on days 3, 7, and 21 after tamoxifen injection in vehicle and antibody-treated mice.
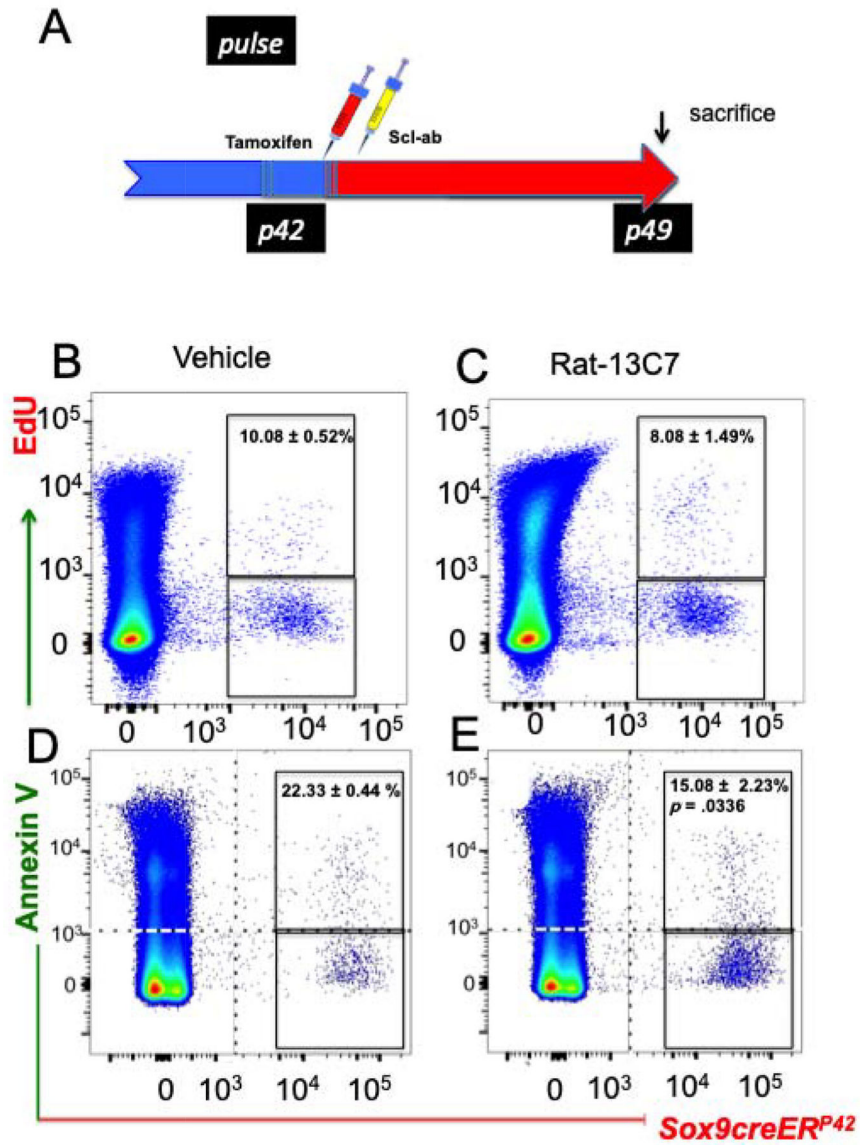
Fig 3.
Blocking antibody to sclerostin suppresses apoptosis without affecting the rate of proliferation in Sox9creER+ multi-potential cells: (*A*) Protocol used in the experiment to study the rate of apoptosis of Sox9-creER+ cells and their descendants. A single dose of tamoxifen was injected at P42. Twenty-four hours later, mice were subjected to vehicle or rat-13C7 antibody against sclerostin protein, once. (*B*, *C*) Representative flow cytometry dot plot analysis showing the fraction of TdTomato+ cells isolated from Sox9-creER; R26RTomato mice and gated on TdTomato+ cells and EdU-alexafluor-488+ cells at 7 days after tamoxifen. (*D*, *E*) Representative dot plot analysis after flow cytometry analysis showing the fraction of TdTomato+ cells from Sox9-creER; R26RTomato mice and gated on TdTomato+ cells and Annexin V-FITC at 7 days after tamoxifen. CD45+ and DAPI+ cells were gated out during analysis.
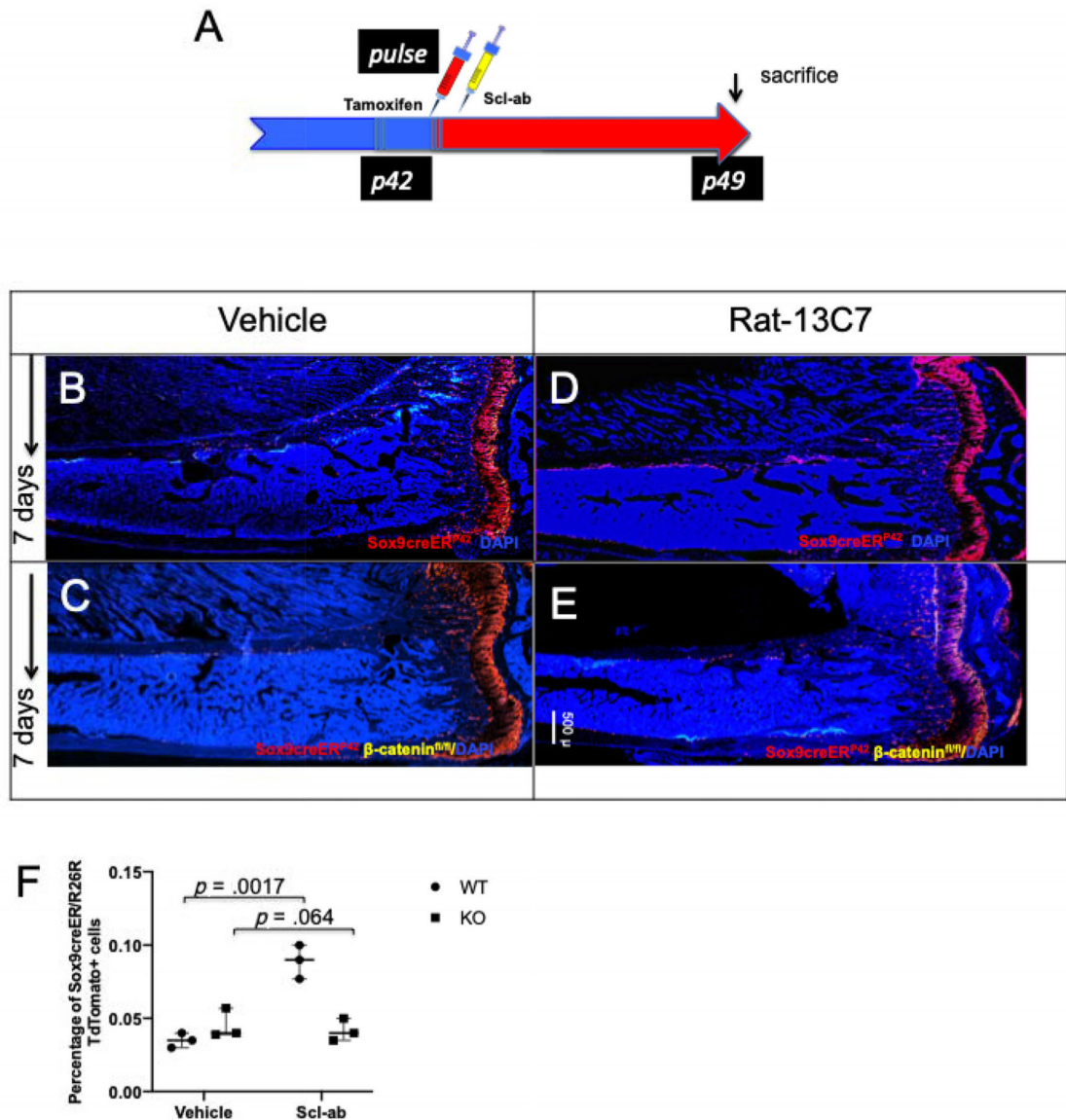
Fig 4.
Deletion of β-catenin leads to complete abrogation of increase in Sox9creER-positive multipotent cells in vivo. (*A*) The protocol used in the experiment to study the rate of apoptosis of Sox9-creER+ cells and their descendants. Mice received a single tamoxifen injection at P42. Twenty-four hours later, mice were subjected to either vehicle or rat-13C7 antibody once weekly in Sox9-creER; R26RTomato and Sox9-creER; R26RTomato; β-catenin$^{fl/fl}$ mice. (*B, D*) Representative long bone section from Sox9creER; R26RTdTomato; mice at 7 days post-tamoxifen administration. (*C, E*) Representative long bone section from Sox9creER; R26RTdTomato; β-catenin$^{fl/fl}$ mice at 7 days post-tamoxifen administration. (*F*) Flow cytometry analysis of tomato cells from Sox9creER; R26RTdTomato; and Sox9creER; R26RTdTomato; β-catenin$^{fl/fl}$ mice. Graph representing the flow cytometry analysis at 7 days after tamoxifen. Statistical evaluation was done by nonparametric two-tailed Student's *t* tests.
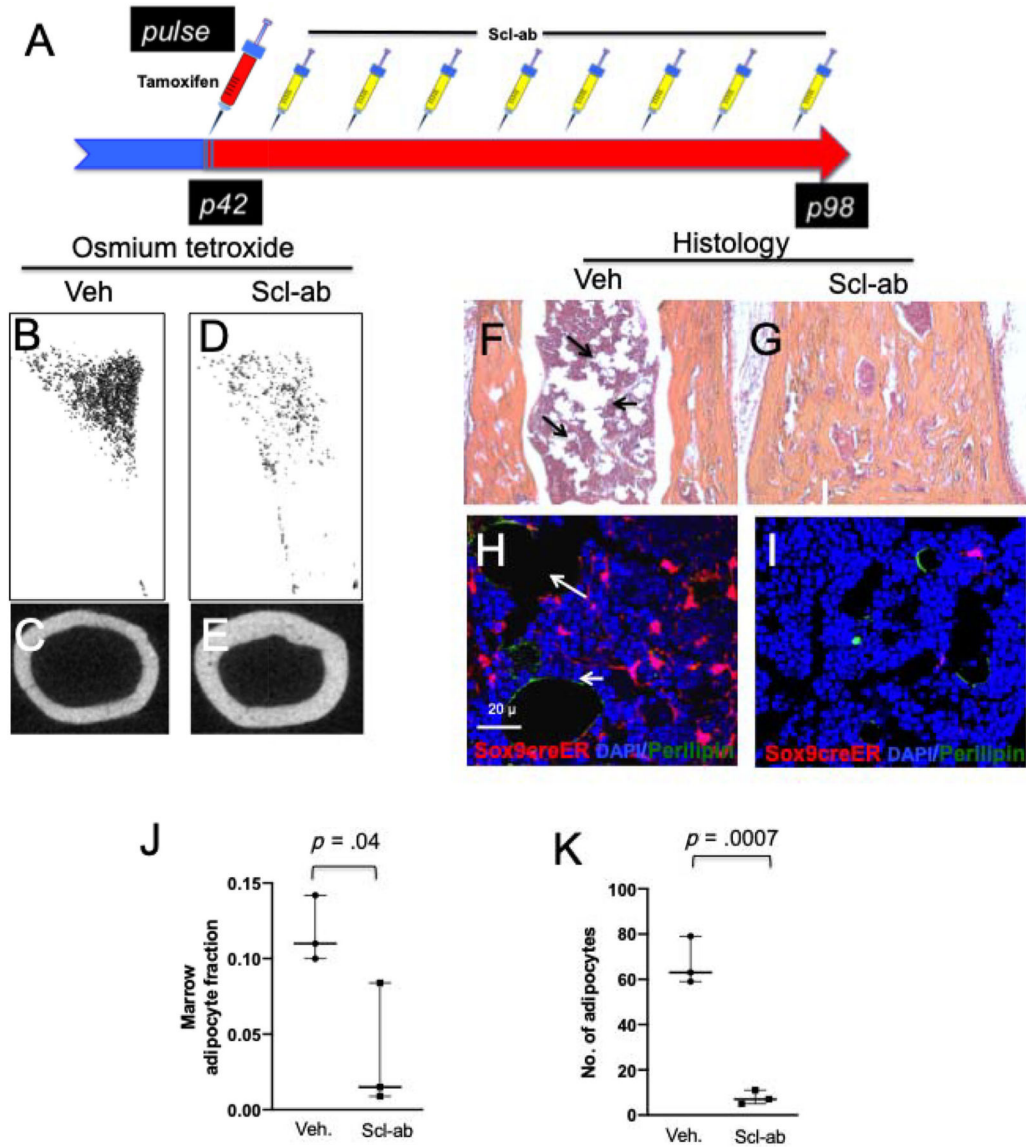
Fig 5.
Scl-ab administration suppresses adipogenic differentiation of Sox9creER+ multipotential cells in vivo. (*A*) The protocol used in the experiment to study the fate of Sox9-creER+ cells after Scl-ab administration. Mice received a single tamoxifen injection at P42. Twenty-four hours later, mice were subjected to either vehicle or Scl-ab once weekly for 8 weeks. Mice were euthanized and long bones were harvested for evaluation by histology, micro-CT, epifluorescence microscopy, and confocal microscopy. (*B, D*) Representative osmium tetroxide staining of micro-CT specimens from the tibia of mice showing adipose tissue in vehicle (*B*) and Scl-ab (*D*) treatment of mice after 8 weeks. (*C, E*) Representative mid-cortical micro-CT image of tibia of vehicle-treated and antibody-treated mice. (*F, G*) H & E image of distal tibias of vehicle- and antibody-treated mice. Note that the abundance of adipocytes in vehicle-treated mice (arrows in *F*) and abundance of mineralized tissue but lack of adipose tissue in antibody-treated mice (*G*). (*H, I*) Confocal images of the distal

tibias show the Sox9creER-R26RTdTomato + adipocytes that overlap with perilipin in vehicle-treated mice compared with antibody-treated mice (right). (*J*) (*K*) Graphs representing the fraction of Sox9creER-R26RTdTomato + cells that is adipocytes and the absolute number of adipocytes counted blindly in the distal tibias of vehicle- and antibody-treated mice.